crystals

MDPI

Article

Gain Properties of the Single Cell of a One-Dimensional Photonic Crystal with PT Symmetry

Piotr Witoński [1,*], Agnieszka Mossakowska-Wyszyńska [1] and Paweł Szczepański [1,2]

[1] Institute of Microelectronics and Optoelectronics, Warsaw University of Technology, Koszykowa 75, 00-665 Warsaw, Poland
[2] National Institute of Telecommunications, Szachowa 1, 04-894 Warsaw, Poland
* Correspondence: piotr.witonski@pw.edu.pl

Abstract: In this paper, an analysis of gain properties of a single primitive cell of a one-dimensional photonic crystal with parity–time symmetry is demonstrated for the first time. The proposed simple model makes it possible to study the transmission and amplification properties of the investigated cell made of a wide range of optical materials, taking into account the refractive index of the surrounding medium. This analysis is carried out with the use of a transfer matrix method. The obtained characteristics allow indicating the optimal size of the studied structure providing wave amplification, i.e., a transmittance greater than unity. In this case, the increase in the wave intensity in the gain layer exceeds its decrease in the loss layer. This effect is illustrated with the distributions of the electromagnetic field of waves propagating inside the cell.

Keywords: photonic crystal; parity–time symmetry; transfer matrix method

Citation: Witoński, P.; Mossakowska-Wyszyńska, A.; Szczepański, P. Gain Properties of the Single Cell of a One-Dimensional Photonic Crystal with PT Symmetry. *Crystals* **2023**, *13*, 258. https://doi.org/10.3390/cryst13020258

Academic Editors: Fu-Der Lai, Mu-Chun Wang and Wen-Ching Hsieh

Received: 11 January 2023
Revised: 27 January 2023
Accepted: 31 January 2023
Published: 2 February 2023

1. Introduction

An investigation of parity–time (PT) symmetric structures began in 1998 with work [1], which showed that even non-Hermitian Hamiltonians can exhibit entirely real spectra as long as they fulfill the conditions of PT symmetry.

In 2007, work [2] initiated the study of optical one-dimensional structures, which are made from the same amount of two artificial materials, amplifying and absorbing, with different refractive indexes. In general, these coefficients are complex $n = n_{Re} + in_{Im}$ and satisfy the condition $n^*(-z) = n(z)$ (the asterisk denotes a complex conjugate). Thus, the PT symmetry is achieved when $n_{Re}(z) = n_{Re}(-z)$ and $n_{Im}(z) = -n_{Im}(-z)$. This implies that the real parts of refractive indices of such materials are equal, and the imaginary parts are equal with respect to their absolute values (i.e., for a gain layer $n_{Im} < 0$ and for a loss layer $n_{Im} > 0$).

PT symmetric structures are investigated in various arrangements: photonic crystals [3], parallel coupling such as PT symmetry lattice [4], optical waveguide networks [5,6], or in lasers as an amplifying medium [7,8]. These structures are being studied for their very intriguing properties: beam refraction [9], nonreciprocity of light propagation [9], unidirectional invisibility [10], and coherent perfect absorption [11]. Such structures are made in the semiconductor III-V technology [8], an example of which is an electron beam lithography process that contains multiple electron beam evaporation steps and inductively-coupled plasma etching [12]. In these devices, the semiconductor junction is the gain layer, and the loss layer is obtained by creating an additional metallic grating [8] or selective doping of Cr/Ge [12].

So far, the literature has not shown a detailed analysis of the distribution of the electromagnetic field in a single cell of a one-dimensional photonic crystal (1-D PC) with PT symmetry, enabling the study of its gain properties. Therefore, this work aims to present an analysis of these properties of such a single primitive cell. This goal is reached by proposing an original simple model, which enables the study of the transmission and amplification

properties of the investigated cell made of any optical material, taking into account the refractive index of the surrounding medium. The property analysis presented in the paper is carried out using a modified transition matrix method [13,14]. An analysis for a PT primitive cell is provided to numerically obtain characteristics showing the reflectances and transmittances, and the electromagnetic field distribution. The study illustrates that an argument of the reflections at all boundaries between the cell layers (gain and loss) and the material surrounding the cell and the cell layers causes the gain layer's amplification of the electromagnetic wave to be higher than the loss layer's attenuation. The next section presents the theory describing the 1-D PC with PT symmetry. In Section 3, the characteristics showing the reflectances and transmittance as a function of the ratio of the grating period to the operating wavelength, and the electromagnetic field longitudinal distributions are demonstrated. Section 4 presents the conclusions.

2. Methods

The structure of an analyzed single cell of a one-dimensional photonic crystal with PT symmetry is presented in Figure 1. Each layer of the cell is characterized by the refractive index n_1 or n_2 and a width w_a or w_b in a gain (the light red background) and a loss (the light blue background) layer, respectively. The length of the investigated cell is denoted by Λ. In the case of the PT cell, it equals $\Lambda_{PT} = w_a + w_b$, where both layers have the same width, i.e., $w_a = w_b$. For the homogeneous gain or loss cell, the length is denoted by $\Lambda_g = w_a$, or $\Lambda_\alpha = w_b$, respectively.

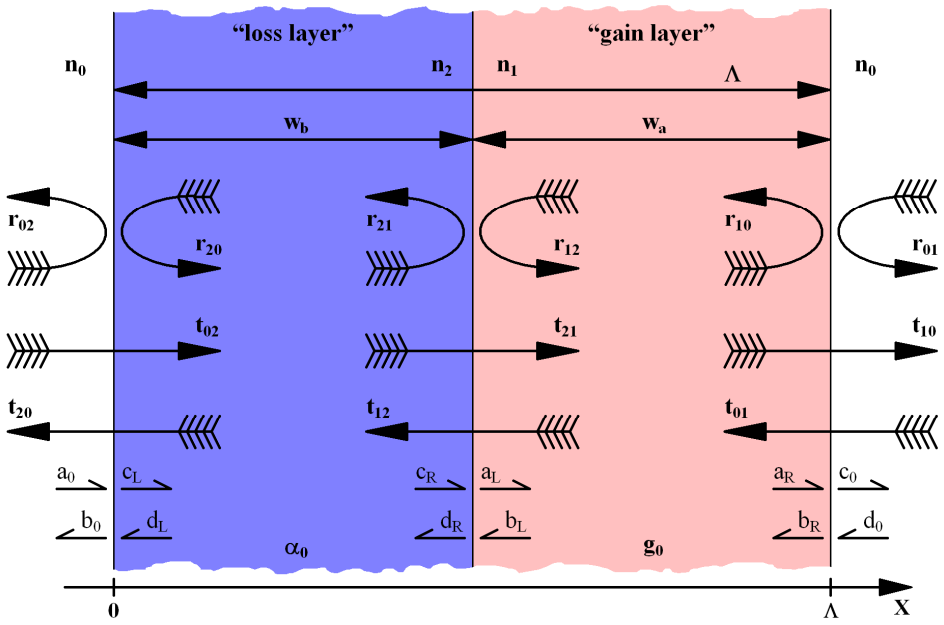

Figure 1. Scheme of the analyzed single primitive cell with PT symmetry.

The refractive indices are complex for both layers and are given by:

$$\begin{aligned} n_1 &= n_{Re} - in_{Im}, \\ n_2 &= n_{Re} + in_{Im}, \end{aligned} \tag{1}$$

where n_{Re} and n_{Im} are the real and imaginary parts of the refractive indices, respectively. The real part n_{Re} characterizes the material from which the investigated structure is made. The imaginary part n_{Im} of a linear single cell is related to a small-signal gain coefficient g_0 for the gain layer and a small-signal loss coefficient α_0 for the loss layer:

$$n_{Im} = |g_0/k_0| = |\alpha_0/k_0|, \tag{2}$$

where k_0 is the wave number in free space. The refractive index of the surrounding medium is denoted by n_0.

The reflection r and transmission t of the light incident on an interface between two optical media layers are complex and described by the following Fresnel equations:

- The interface between the gain layer and the surrounding medium:

$$r_{10} = \frac{n_1 - n_0}{n_1 + n_0},\ r_{01} = \frac{n_0 - n_1}{n_0 + n_1},\ t_{10} = \frac{2n_1}{n_1 + n_0},\ t_{01} = \frac{2n_0}{n_0 + n_1}, \tag{3}$$

- The interface between the loss and gain layers:

$$r_{21} = \frac{n_2 - n_1}{n_2 + n_1},\ r_{12} = \frac{n_1 - n_2}{n_1 + n_2},\ t_{21} = \frac{2n_2}{n_2 + n_1},\ t_{12} = \frac{2n_1}{n_1 + n_2}, \tag{4}$$

- The interface between the surrounding medium and the loss layer:

$$r_{02} = \frac{n_0 - n_2}{n_0 + n_2},\ r_{20} = \frac{n_2 - n_0}{n_2 + n_0},\ t_{02} = \frac{2n_0}{n_0 + n_2},\ t_{20} = \frac{2n_2}{n_2 + n_0}. \tag{5}$$

The electric field distribution within the gain layer $E_1(x)$ and the loss layer $E_2(x)$ can be expressed as a sum of a right-going plane wave (positive direction of the X axis) and a left-going plane wave (negative direction of the X axis), where each wave has a complex amplitude. According to [14], they can be written down as:

$$\begin{aligned} E_1(x) &= a \cdot e^{(ik_0 n_1 x)} + b \cdot e^{(-ik_0 n_1 x)}, \\ E_2(x) &= c \cdot e^{(ik_0 n_2 x)} + d \cdot e^{(-ik_0 n_2 x)}, \end{aligned} \tag{6}$$

where a and b are the electric field complex amplitudes of waves travelling in opposite directions in the gain layer, and c and d are the electric field complex amplitudes of waves traveling in opposite directions in the loss layer. The amplitudes of waves close to the interface between the different layers are as follows:

- The gain layer and the surrounding medium—a_R and b_R in the gain layer, and c_0 and d_0 in the surrounding medium;
- The loss and gain layers—c_R and d_R in the loss layer, and a_L and b_L in the gain layer;
- The surrounding medium and the loss layer—a_0 and b_0 in the surrounding medium, and c_L and d_L in the loss layer.

The investigated PT symmetry cell is examined with the help of the modified transfer matrix method [13,14]:

$$\begin{bmatrix} a_0 \\ b_0 \end{bmatrix} = M \cdot \begin{bmatrix} c_0 \\ d_0 \end{bmatrix} \tag{7}$$

and the total transfer matrix M of this cell has the following form:

$$M = J_{02} P_2 J_{21} P_1 J_{10}, \tag{8}$$

where J are the matrices describing the behavior of the electromagnetic wave at the interface between:

- The gain layer and the surrounding medium:

$$J_{10} = \frac{1}{t_{10}} \cdot \begin{bmatrix} 1 & -r_{01} \\ r_{10} & t_{01} \cdot t_{10} - r_{01} \cdot r_{10} \end{bmatrix}, \tag{9}$$

- The loss and gain layers:

$$J_{21} = \frac{1}{t_{21}} \cdot \begin{bmatrix} 1 & -r_{12} \\ r_{21} & t_{12} \cdot t_{21} - r_{12} \cdot r_{21} \end{bmatrix}, \tag{10}$$

- The surrounding medium and the loss layer:

$$J_{02} = \frac{1}{t_{02}} \cdot \begin{bmatrix} 1 & -r_{20} \\ r_{02} & t_{20} \cdot t_{02} - r_{20} \cdot r_{02} \end{bmatrix}. \tag{11}$$

The matrices P_1 and P_2 describe the wave propagation through the gain and loss layer, respectively:

$$P_1 = \begin{bmatrix} e^{-ik_0 n_1 w_a} & 0 \\ 0 & e^{ik_0 n_1 w_a} \end{bmatrix}, \; P_2 = \begin{bmatrix} e^{-ik_0 n_2 w_b} & 0 \\ 0 & e^{ik_0 n_2 w_b} \end{bmatrix}. \tag{12}$$

The field amplitudes of waves at the interface between two different media in the PT primitive cell are related in the following way:

$$\begin{bmatrix} a_0 \\ b_0 \end{bmatrix} = J_{02} \cdot \begin{bmatrix} c_L \\ d_L \end{bmatrix}, \; \begin{bmatrix} c_L \\ d_L \end{bmatrix} = P_2 \cdot \begin{bmatrix} c_R \\ d_R \end{bmatrix}, \; \begin{bmatrix} c_R \\ d_R \end{bmatrix} = J_{21} \cdot \begin{bmatrix} a_L \\ b_L \end{bmatrix}, \; \begin{bmatrix} a_L \\ b_L \end{bmatrix} = P_1 \cdot \begin{bmatrix} a_R \\ b_R \end{bmatrix}, \; \begin{bmatrix} a_R \\ b_R \end{bmatrix} = J_{10} \cdot \begin{bmatrix} c_0 \\ d_0 \end{bmatrix}. \tag{13}$$

Using components of the total transfer matrix M, a related scattering matrix S is defined as follows:

$$S = \frac{1}{M_{11}} \cdot \begin{bmatrix} M_{21} & M_{21} \cdot M_{11} - M_{12} \cdot M_{21} \\ 1 & -M_{12} \end{bmatrix} = \begin{bmatrix} r_{PT\alpha} & t_{PT} \\ t_{PT} & r_{PTg} \end{bmatrix} \tag{14}$$

where the reflections $r_{PT\alpha}$ and r_{PTg}, and the transmission t_{PT} coefficients of the whole cell are complex. In general, the two reflectances and transmittance are related to the reflections $r_{PT\alpha}$ and r_{PTg}, and transmission t_{PT} coefficients in the following way:

$$R_{PT\alpha} = |r_{PT\alpha}|^2, \; R_{PTg} = \left|r_{PTg}\right|^2, \; T_{PT} = |t_{PT}|^2. \tag{15}$$

The eigenvalues λ_1 and λ_2 of the S matrix are the solutions of the characteristic equation $det(S - \lambda_e I) = 0$, where I is an identity matrix and λ_e is an eigenvalue vector [15], and are described as follows:

$$\lambda_{1,2} = \frac{1}{2}\left(r_{PT\alpha} + r_{PTg} \pm \sqrt{r_{PT\alpha}^2 + r_{PTg}^2 + 4t_{PT}^2 - 2r_{PT\alpha}r_{PTg}}\right). \tag{16}$$

The obtained eigenvalues allow to determine whether a given PT cell satisfies the PT symmetry conditions [16,17]. In a PT symmetric phase, the eigenvalues λ_1 and λ_2 are unimodular, i.e., $|\lambda_1| = |\lambda_2| = 1$. For such an operating mode, the PT operation maps each scattering eigenstate back to itself. However, in a broken symmetry phase with reciprocal moduli of eigenvalues, i.e., $|\lambda_1| = 1/|\lambda_2|$, $|\lambda_1| < 1$, $|\lambda_2| > 1$, each scattering eigenstate is mapped to the other.

In order to describe the lasing threshold in the examined PT symmetric cell, the condition for reproducing the wave (its amplitude and phase) after its full circulation through the structure should be written as:

$$c_L = d_L \cdot r_{20}. \tag{17}$$

After taking into account the appropriate dependencies for the reflection coefficients and the field amplitudes (Equations (5) and (12) respectively), the following transcendental dependence is obtained:

$$e^{-ik_0(n_1+n_2)\frac{\Lambda_{PT}}{2}} - r_{12}r_{10}e^{ik_0(n_1-n_2)\frac{\Lambda_{PT}}{2}} = r_{21}r_{20}e^{-ik_0(n_1-n_2)\frac{\Lambda_{PT}}{2}} + r_{10}r_{20}(t_{12} \cdot t_{21} - r_{12} \cdot r_{21})e^{ik_0(n_1+n_2)\frac{\Lambda_{PT}}{2}} \tag{18}$$

In Equation (18), all reflection and transmission coefficients and refractive indices are complex.

In the case of the homogeneous gain cell, Equation (17) is simplified to the following form:

$$a_L = b_L \cdot r_{10} \;\Rightarrow\; e^{-ik_0 n_1 \Lambda_g} = r_{10}^2 e^{ik_0 n_1 \Lambda_g}. \tag{19}$$

The integral mean of the PT cell's intensity was introduced to compare its electric field longitudinal distribution. Such mean is obtained for both layers of the PT cell separately, i.e., for the gain layer $\|E_1(x)\|$ and the loss layer $\|E_2(x)\|$, and has the following form:

$$\|E_1(x)\| = \frac{1}{w_a}\int_{w_a}\left(|a(x)|^2 + |b(x)|^2\right)dx,\ \|E_2(x)\| = \frac{1}{w_b}\int_{w_b}\left(|c(x)|^2 + |d(x)|^2\right)dx. \tag{20}$$

The characteristics showing the eigenvalues, reflectances and transmittances as a function of the ratio of the grating period to the operating wavelength, and the electromagnetic field longitudinal distribution are presented in the next section.

3. Results and Discussion

Numerical analysis of the single cell of a one-dimensional photonic crystal with PT symmetry is performed with the assumption that the refractive index's real part is equal to n_{Re} = 3.165 for a semiconductor material InP [18], and the imaginary part is n_{Im} = 0.1 [7,15,17]. The analyzed cell is surrounded by air, i.e., the refractive index is n_0 = 1. The wavelength is λ = 1.55 µm (the third telecommunication window). Moreover, the PT structure is only excited by the wave from one side. Performing the calculations requires the assumption of a steady state, i.e., the fulfillment of the modified transfer matrix method—Equation (7).

The reflection and transmission complex coefficients for the investigated PT cell were determined at all boundaries between the cell layers (gain and loss) and the material surrounding the cell. Table 1 presents the moduli and arguments of these coefficients obtained from Equations (3)–(5); the light blue background indicates the coefficients in the loss layer, and the light red one in the gain layer.

Table 1. Moduli and arguments of reflection and transmission coefficients.

Coefficient	Modulus	Argument [πrad]
r_{02}	0.5202	−0.9929
t_{02}	0.4801	−0.0076
t_{20}	1.5201	0.0024
r_{20}	0.5202	0.0071
r_{21}	0.0316	0.5000
t_{21}	1.0005	0.0101
t_{12}	1.0005	−0.0101
r_{12}	0.0316	−0.5000
r_{10}	0.5202	−0.0071
t_{10}	1.5201	−0.0024
t_{01}	0.4801	0.0076
r_{01}	0.5202	0.9929

It is worth noting that, at the boundary between the layers forming the PT cell, the reflection coefficients are negligibly small and the transmission coefficients are dominant and equal unity. Moreover, the arguments of the reflection and transmission complex coefficients in the gain layer are negative, whereas in the loss layer they are positive. This behavior of the coefficient arguments is caused by the differences between the imaginary parts of the refractive index of both layers forming the PT cell.

3.1. Eigenvalues of the S Matrix

To indicate whether the investigated cell meets the conditions of the PT symmetric phase, it is necessary to analyze the eigenvalues λ_1 and λ_2 (see Equation (16)) as a function of a ratio of the length of the PT cell to the operating wavelength Λ_{PT}/λ, see Figure 2.

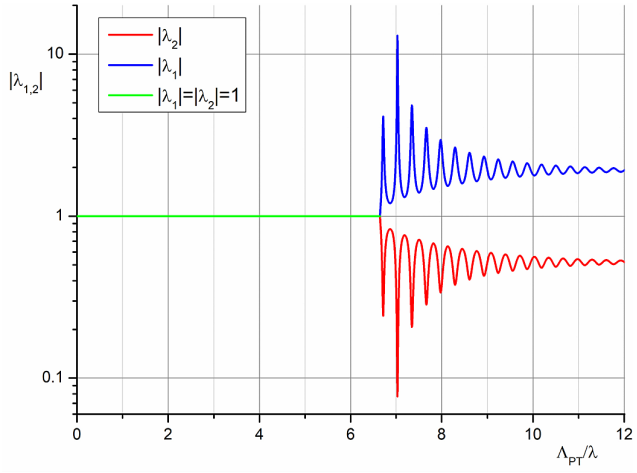

Figure 2. Eigenvalues λ_1 and λ_2 as a function of ratio Λ_{PT}/λ.

The eigenvalues λ_1 and λ_2 are unimodular for small values of Λ_{PT}/λ. After reaching the point Λ_{PT}/λ = 6.650, bifurcation occurs and the eigenvalues have reciprocal moduli. The value of the mentioned point is consistent with the work [19], where the condition for the unimodular eigenvalues of the S matrix is shown as a function of the reflection and transmission coefficients (see Equation (10) in [19]). For larger values of Λ_{PT}/λ, the investigated eigenvalues indicate that symmetry has been broken.

3.2. Reflectance and Transmittance

To examine the reflectance and transmittance of the PT cell, Equation (15) is used. The figures showing the reflectances and the transmittances as functions of the ratio of the length of the cell to the operating wavelength Λ/λ, calculated for the independent gain and loss cells, and the entire PT structure, are presented below (see Figures 3 and 4).

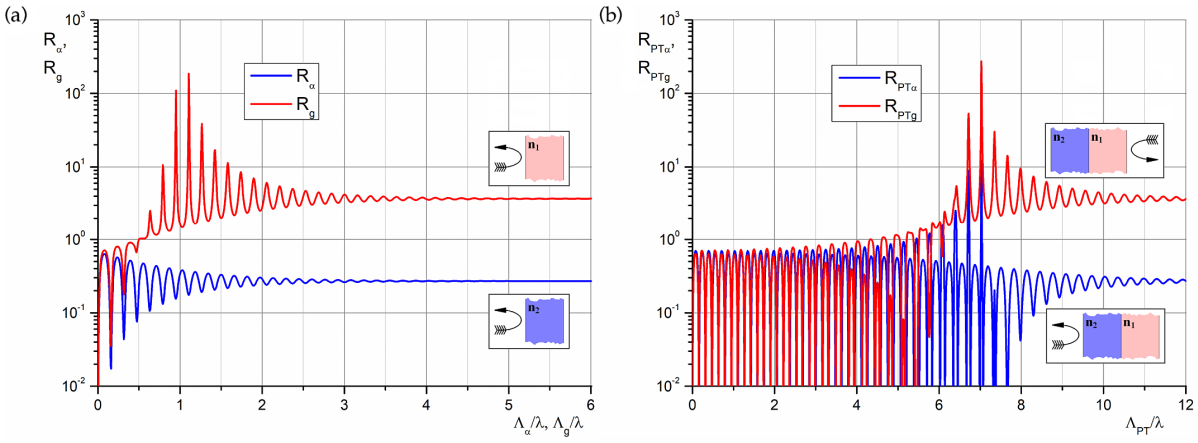

Figure 3. Reflectance as a function of ratio Λ/λ for: (**a**) independent gain R_g and loss R_α cells; (**b**) PT gain layer R_{PTg} and PT loss layer $R_{PT\alpha}$.

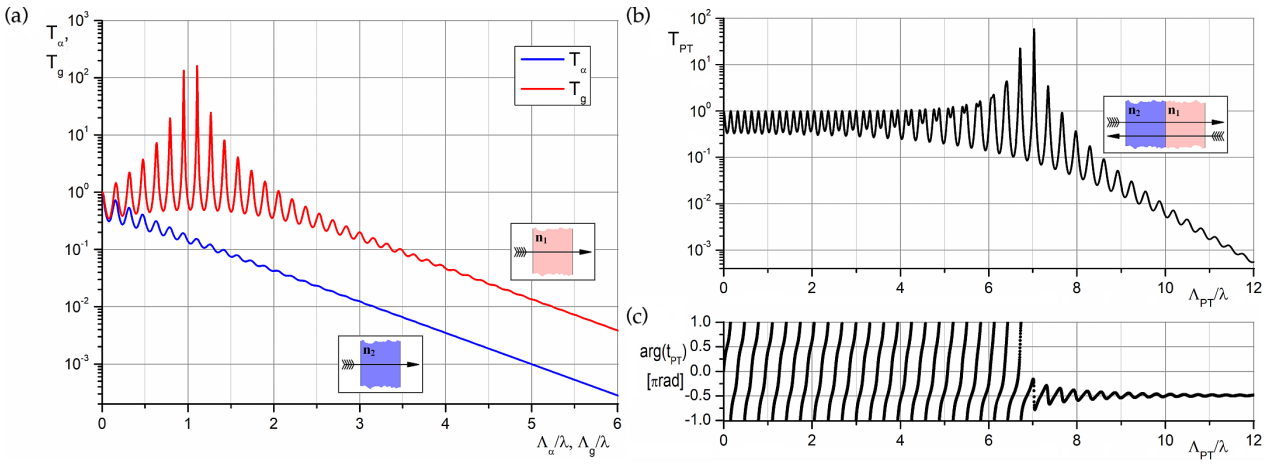

Figure 4. Transmittance as a function of ratio Λ/λ for: (**a**) independent gain T_g and loss T_α cells; (**b**) PT cell T_{PT}. (**c**) Argument of transmission coefficient t_{PT} as a function of ratio Λ_{PT}/λ.

Figure 3 shows the reflectance of the homogeneous (gain or loss) media and the PT cell. In the calculation, it was assumed that the entire PT cell is two times bigger than the homogeneous cell.

In general, oscillations are observed in the characteristics, and they result from the constructive and destructive interferences of the counter running waves inside the cell. For the larger values of the ratio Λ/λ, the oscillations become smaller due to the increasing difference between the intensities of these waves.

In the case of the homogeneous loss cell (see Figure 3a), as the ratio Λ_α/λ increases, the reflectance R_α (blue line) decreases and the oscillations disappear. For the larger Λ_α/λ (i.e., for the larger cell size), the waves inside the loss cell are more strongly damped. In this situation, the reflectance will depend only on the Fresnel reflection from the boundary of the media r_{02} (determined by the refractive indices' contrast between n_0 and n_2).

For the homogeneous gain cell (see Figure 3a), as the ratio Λ_g/λ increases, the reflectance R_g (red line) also increases up to the maximal value at a point of a lasing threshold $\Lambda_g/\lambda = 1.107$ obtained from Equation (19). In such circumstances, the waves inside the gain cell are more strongly amplified. At the point of a lasing threshold, the total gain of the waves in the cell is equal to the total loss (the outcoupled waves). For values of the ratio Λ_g/λ above the lasing point, the wave entering the structure must be growing larger to maintain the steady state. In this situation, the waves propagating inside the gain cell are suppressed by interference with the entering wave. This effect is observed in Figure 3a as decreasing of the reflectance R_g, which tends to the value of reflectance being equal to the inverse of the Fresnel formula for r_{10} [16].

Figure 3b presents the reflectances of the PT cell for the loss layer $R_{PT\alpha}$ (blue line) and the gain layer R_{PTg} (red line). In the case of the loss layer, the reflectance $R_{PT\alpha}$ is less than unity for the ratio Λ_{PT}/λ, smaller than around $\Lambda_{PT}/\lambda = 5.4$. However, the reflectance $R_{PT\alpha}$ demonstrates six maxima exceeding unity for bigger values of Λ_{PT}/λ. The highest reflectance occurs around the point of the lasing threshold $\Lambda_{PT}/\lambda = 7.032$, obtained from Equation (18). As the ratio Λ_{PT}/λ increases, the reflectance above the mentioned point is less than unity and decreases towards the Fresnel reflection value r_{02}. In the case of the gain layer, with increasing of the ratio Λ_{PT}/λ, the reflectance R_{PTg} oscillates up to the lasing point, where it reaches a maximum value. For larger values of Λ_{PT}/λ, the reflectance R_{PTg} decreases to a value of the inverse of the Fresnel formula for r_{10}.

The transmittances for the independent gain and loss cells, and the PT structure, are demonstrated in Figure 4. All presented characteristics of the transmittances exhibit oscillations. In the case of the homogeneous loss cell (see Figure 4a), as the ratio Λ_α/λ increases, the transmittance T_α (blue line) tends to zero and the oscillations disappear. The reason for such behavior is the same as for the diminishing of the reflectance R_α. In the case

of the homogeneous gain cell (see Figure 4a), the transmittance T_g (red line) oscillates and increases until reaching a maximum value at the point of the lasing threshold. For larger values of the ratio Λ_g/λ, it decreases towards zero and the oscillations vanish. The waves propagating inside the gain cell, above the lasing point, are suppressed by interference with the incident wave, thus the transmittance tends to zero.

The transmittance T_{PT} for the PT cell is shown in Figure 4b. For the ratio Λ_{PT}/λ smaller than $\Lambda_{PT}/\lambda = 4$, the transmittance maxima values slightly exceed unity. For the ratio range between $\Lambda_{PT}/\lambda = 4$ and $\Lambda_{PT}/\lambda = 6.650$, the magnitude of successive maxima increases and the PT cell demonstrates gain properties. Simultaneously, the investigated structure satisfies the PT symmetry conditions below $\Lambda_{PT}/\lambda = 6.650$. For further increasing of the ratio Λ_{PT}/λ, up to the point of the lasing threshold $\Lambda_{PT}/\lambda = 7.032$, the PT symmetry is broken and the magnitude of the observed maxima increases. In this situation, the PT cell continues demonstrating the gain properties. At the point of the lasing threshold, the transmittance T_{PT} reaches a maximal value and the PT structure has the highest gain properties. For the larger PT cell size (i.e., for the larger ratio Λ_{PT}/λ), the PT symmetry is broken, the transmittance T_{PT} decreases towards zero and its oscillations reduce. Thus, the increase in the wave intensity caused by passing through the gain layer is lost during its travel through the loss layer.

Equation (14) is used to obtain the complex transmission coefficient t_{PT}. Figure 4c shows an argument of this transmission coefficient $arg(t_{PT})$ as a function of the ratio Λ_{PT}/λ. The periodic variations of the argument of the transmission are observed for the ratio Λ_{PT}/λ smaller than its value at the point of the lasing threshold $\Lambda_{PT}/\lambda = 7.032$. The argument's oscillations disappear and the argument tends to a constant value for the greater ratio Λ_{PT}/λ (above the lasing point). This value is the constant difference between the input and output waves' phases of the PT cell.

3.3. Electromagnetic Field Distribution

The longitudinal field distribution in the investigated PT cell is calculated using Equations (6)–(13) with the following assumptions: the PT cell is only illuminated from one side with a wave of intensity $I_{inc} = |a_0|^2$, the intensity of the reflected wave from the same side is $I_{ref} = |b_0|^2$, output intensity equals $I_{out} = |c_0|^2 = 1$ W/cm^2, and simultaneously $d_0 = 0$. This distribution is calculated in two steps. In the first one, the intensity values of the incident wave I_{inc} and reflected wave I_{ref} from the same side are obtained using the transfer matrix method with the assumed value of the output wave intensity I_{out}. In the second step, the field distributions in each layer are calculated as a function of the X-coordinate according to Figure 1.

Figures 5 and 6 present the obtained characteristics of the longitudinal field distribution: the amplitudes ($|a_0|$, $|b_0|$, $|c|$, $|d|$, $|a|$, $|b|$, $|c_0|$) and phases ($\varphi(a_0)$, $\varphi(b_0)$, $\varphi(c)$, $\varphi(d)$, $\varphi(a)$, $\varphi(b)$, $\varphi(c_0)$) of the counter running waves versus the position in the PT cell.

Figure 5 presents the field distribution for the ratio $\Lambda_{PT}/\lambda = 0.158$. It is the smallest value of the ratio Λ_{PT}/λ for which the first peak of the transmittance greater than unity occurs (Figure 4b), and the investigated structure satisfies the PT symmetry conditions. In particular, Figure 5a,b shows the amplitudes and Figure 5c,d shows the phases of the longitudinal field distribution. The characteristics placed in the left column were obtained for the PT cell illuminated from the loss layer, while the characteristics in the right column were obtained for the PT cell illuminated from the gain layer.

As shown in Figure 5a,b, in the gain layer, the amplitudes of the propagating waves are amplified (amplitude $|a|$ in the positive direction of the X axis—red line, and amplitude $|b|$ in the negative direction of the X axis—pink line) as expected. The opposite situation is observed in the loss layer, where the amplitudes of the propagating waves are suppressed (amplitude $|c|$ in the positive direction of the X axis—blue line, and amplitude $|d|$ in the negative direction of the X axis—cyan line). Comparing the behavior of the field distribution in oppositely oriented single PT cells, for the assumed intensity I_{out} (green line), shows that the incident wave amplitudes are the same (orange line). Simultaneously, the

amplitudes of the reflected waves (dark yellow line) are marginally different and the wave reflected from the loss layer is greater, which is consistent with the reflectance's distribution (see Figure 3b).

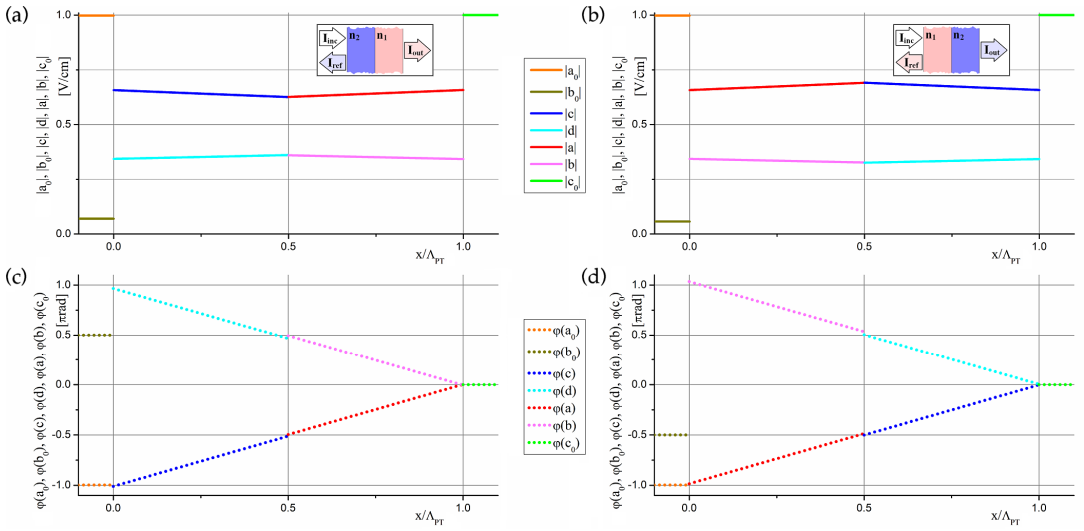

Figure 5. Longitudinal field distribution (amplitude and phase) of counter running waves versus position in the PT cell for $\Lambda_{PT}/\lambda = 0.158$ (**a,b**) amplitudes of field $|a_0|$, $|b_0|$, $|c|$, $|d|$, $|a|$, $|b|$, $|c_0|$; (**c,d**) phases of field $\varphi(a_0)$, $\varphi(b_0)$, $\varphi(c)$, $\varphi(d)$, $\varphi(a)$, $\varphi(b)$, $\varphi(c_0)$. Characteristics in the left column—PT cell illuminated from the loss layer; right column—PT cell illuminated from the gain layer.

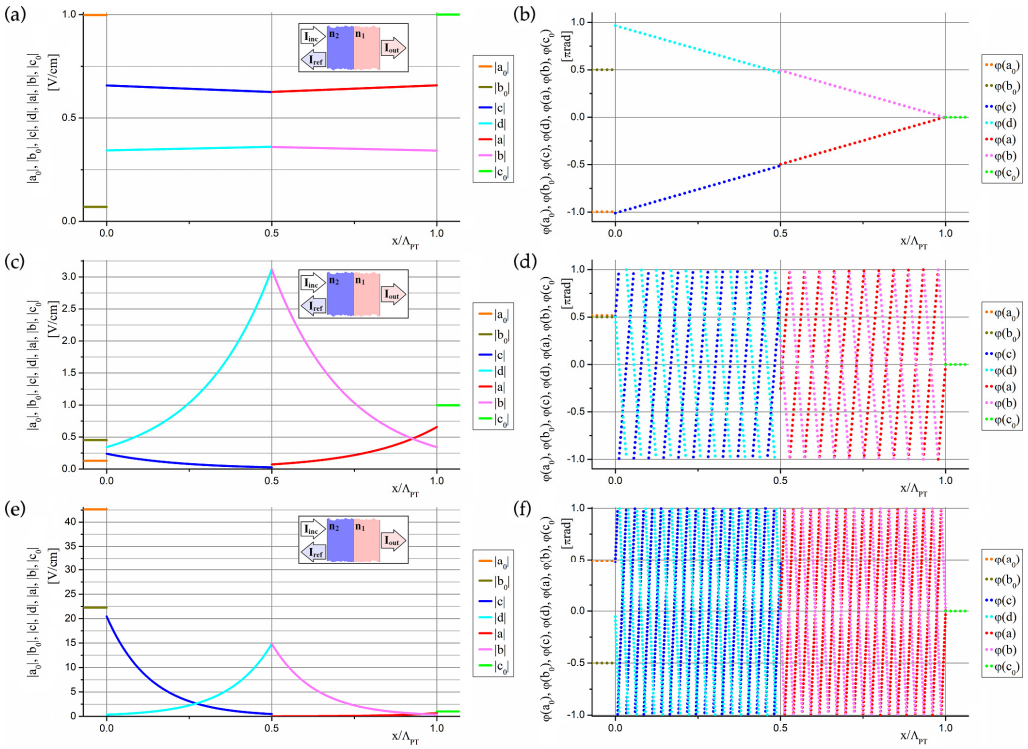

Figure 6. Longitudinal field distribution (amplitude and phase) of counter running waves versus position in the PT cell illuminated from the loss layer for: (**a,b**) $\Lambda_{PT}/\lambda = 0.158$; (**c,d**) $\Lambda_{PT}/\lambda = 7.032$; (**e,f**) $\Lambda_{PT}/\lambda = 12.0$. Characteristics in the left column—amplitudes of field $|a_0|$, $|b_0|$, $|c|$, $|d|$, $|a|$, $|b|$, $|c_0|$; right column—phases of field $\varphi(a_0)$, $\varphi(b_0)$, $\varphi(c)$, $\varphi(d)$, $\varphi(a)$, $\varphi(b)$, $\varphi(c_0)$.

Moreover, comparing the behavior of the wave phases in both single PT cells (illuminated from different layers; see Figure 5c,d), for the assumed value of the phase of the

output wave $\varphi(c_0) = 0$ (green dotted line), shows that the phases of the input waves (orange dotted line) are equal. On the other hand, the phases of the reflected waves (dark yellow dotted line) differ exactly by π, which results from the interaction of the wave with the entire PT cell. At the same time, the phases of the waves propagating through the loss and the gain layers change monotonically. The step change of the mentioned phases, caused by a change in refractive index, is observed on the border between the different media.

In the case of the wave reflection from the boundary between two different media with the real indices of refraction, the reflected wave does not change its phase (when the wave is incident from a high to a low refractive index medium) or changes it by π (when the wave is incident from a low to a high refractive index medium). The behavior of the phases between the wave incident on and reflected off the same layer of the PT cell (Figure 5c,d, respectively) is different than in the case of media with the real indices of refraction. When the PT cell is illuminated from the loss layer, the phases differ by $3\pi/2$ (see Figure 5c). In the case of the PT cell illuminated from the gain layer, the phases differ by $\pi/2$ (see Figure 5d). These phase values are related to the interaction of the incident wave with the entire PT cell.

In Figure 6, when the PT cell is only illuminated from the loss layer, the field distribution is presented for three different values of the ratio of the length of the PT cell to the operating wavelength Λ_{PT}/λ:

- The smallest value, for which the first peak of the transmittance greater than unity occurs $\Lambda_{PT}/\lambda = 0.158$ (Figure 6a,b), and the PT cell satisfies the PT symmetry conditions;
- The value at the point of the lasing threshold, when the highest reflectance and transmittance occurs, $\Lambda_{PT}/\lambda = 7.032$ (Figure 6c,d), and the PT symmetry is broken;
- The value, for which the transmittance is lower than 10^{-3}, $\Lambda_{PT}/\lambda = 12.0$ (Figure 6e,f), and the PT symmetry is broken.

Characteristics placed in the left column present the amplitudes of the longitudinal field distribution, while the phases are presented in the right column. The individual amplitudes and phases of the waves are marked with the same colors as in the previous figure.

In general, the distributions of field amplitudes inside the layers of the PT cell are of the same nature as shown in Figure 5. The increase in the ratio Λ_{PT}/λ causes much greater changes in the waves' amplitudes. Moreover, for the assumed I_{out} value, increasing the size of the PT cell (i.e., the ratio Λ_{PT}/λ) causes non-linear changes in the incident and reflected waves. In particular, for the smallest value of $\Lambda_{PT}/\lambda = 0.158$ (see Figure 6a), the incident wave's amplitude is smaller than the reflected one's. In this situation, the transmittance is slightly greater than unity and the whole PT cell amplifies an electromagnetic wave. In the case of the point of the lasing threshold ($\Lambda_{PT}/\lambda = 7.032$) (see Figure 6c), the reflected wave's amplitude is greater than the incident one's. The PT cell amplifies the electromagnetic wave the most, because the transmittance and reflectance are the highest in this case (see Figures 3b and 4b).

Additionally, the whole PT cell acts as a single gain layer, and the transmittance and reflectance are greater than unity simultaneously (see Figures 3a and 4a). In the third case of the ratio Λ_{PT}/λ's value ($\Lambda_{PT}/\lambda = 12.0$) (see Figure 6e), the reflected wave's amplitude is smaller than the incident one's, and the transmitted wave's amplitude is smaller than the incident wave's and reflected wave's amplitudes. Thus, the whole PT cell acts as a single loss layer, and the transmittance and reflectance are much lower than unity simultaneously (see Figures 3a and 4a).

Taking the dependence of the wave's phase on the ratio Λ_{PT}/λ into consideration, the results show that progressively more halves of the propagating wavelength are included in the analyzed PT cell when increasing the ratio. In particular, for the smallest investigated ratio (see Figure 6b), there is only one half of the wavelength in the PT cell. For the higher values of the ratio Λ_{PT}/λ, there are noticeably more halves of the wavelength (see Figure 6d,f).

Further, for the assumed value of the output wave's phase, the difference between the phases of the incident and reflected waves has the following values for the indicated

ratios: Λ_{PT}/λ = 0.158—the phases differ by $3\pi/2$ (see Figure 6b), Λ_{PT}/λ = 7.032—the phases are almost the same (see Figure 6d), Λ_{PT}/λ = 12.0—the phases differ by π (see Figure 6f). In the last two cases, the phase differences mentioned above have values close to the differences that occur when analyzing the incident and reflected waves in materials with real refractive indices.

The expression for the integral mean (Equation (20)) was used to investigate the gain properties of the analyzed PT cell. The integral mean of the intensity of the electric field's longitudinal distribution of each PT layer was calculated using this formula. The obtained results are presented in Table 2 for different values of the ratio Λ_{PT}/λ, as shown in Figure 6.

Table 2. The integral mean of intensity of field distribution in each layer [W/cm^2].

Λ_{PT}/λ	Loss Layer	Gain Layer
0.158	0.535057	0.535126
7.032	2.186726	2.269591
12.0	84.567893	29.266907

In general, for the ratio value smaller or equal to Λ_{PT}/λ at the point of the lasing threshold, the integral mean of the intensity of the electric field is greater in the gain layer than in the loss one (see Table 2, where larger mean values are indicated in light orange). As a result, the entire PT cell demonstrates gain properties, which are related to the values of the reflection and transmission coefficients (see Table 1). The differences in the investigated integral means between the loss and the gain layers are small, but the typical PT structures are made of many elementary cells, which leads to the enhancement of this effect. Further increasing of the ratio Λ_{PT}/λ beyond the point of the lasing threshold causes the structure to lose its gain properties. It begins to strongly absorb the wave, which is confirmed by a very large difference in the integral means for Λ_{PT}/λ = 12.0 between the loss and the gain layers.

4. Conclusions

This work shows the analysis of the gain properties of a single primitive cell of a one-dimensional photonic crystal with parity–time symmetry. In particular, the reflectance and transmittance were obtained for a wide range of the ratio of the PT cell's length to the operating wavelength. The gain properties of such a PT cell occur when the transmittance is greater than unity. This effect is strongly dependent on the length of the PT cell and is the strongest for the length related to the point of the lasing threshold. A longer PT cell loses its gain properties. Moreover, it is shown that the gain properties are caused by the phases of the reflections at the boundary between two different media. This effect is illustrated with the distributions of the electromagnetic field of waves propagating inside the cell and calculated values of the integral mean of the electric field's intensity of each PT layer. The presented model of the PT cell can help in the design of the telecommunication system's elements.

Author Contributions: Conceptualization, P.W. and A.M.-W.; methodology, P.W., A.M.-W. and P.S.; software, P.W.; formal analysis, P.W. and A.M.-W.; investigation, P.W. and A.M.-W.; writing—original draft preparation, P.W. and A.M.-W.; writing—review and editing, P.S.; and visualization, P.W. and A.M.-W. All authors have read and agreed to the published version of the manuscript.

Funding: Warsaw University of Technology.

Data Availability Statement: Not applicable.

Acknowledgments: The authors wish to thank Urszula Wyszyńska for checking the linguistic correctness of the manuscript.

Conflicts of Interest: The authors declare no conflict of interest. The funders had no role in the design of the study; in the collection, analyses, or interpretation of data; in the writing of the manuscript; or in the decision to publish the results.

References

1. Bender, C.M.; Boettcher, S. Real Spectra in Non-Hermitian Hamiltonians Having PT Symmetry. *Phys. Rev. Lett.* **1998**, *80*, 5243–5246. [CrossRef]
2. El-Ganainy, R.; Makris, K.G.; Christodoulides, D.N.; Musslimani, Z.H. Theory of Coupled Optical PT-Symmetric Structures. *Opt. Lett.* **2007**, *32*, 2632–2634. [CrossRef]
3. Longhi, S. Bloch Oscillations in Complex Crystals with PT Symmetry. *Phys. Rev. Lett.* **2009**, *103*, 123601. [CrossRef]
4. Miri, M.-A.; Regensburger, A.; Peschel, U.; Christodoulides, D.N. Optical Mesh Lattices with PT Symmetry. *Phys. Rev. A* **2012**, *86*, 023807. [CrossRef]
5. Suchkov, S.V.; Sukhorukov, A.A.; Huang, J.; Dmitriev, S.V.; Lee, C.; Kivshar, Y.S. Nonlinear Switching and Solitons in PT-symmetric Photonic Systems. *Laser Photonics Rev.* **2016**, *10*, 177–213. [CrossRef]
6. Wu, J.; Yang, X. Ultrastrong Extraordinary Transmission and Reflection in PT-Symmetric Thue-Morse Optical Waveguide Networks. *Opt. Express* **2017**, *25*, 27724. [CrossRef] [PubMed]
7. Feng, L.; Wong, Z.J.; Ma, R.-M.; Wang, Y.; Zhang, X. Single-Mode Laser by Parity-Time Symmetry Breaking. *Science* **2014**, *346*, 972–975. [CrossRef] [PubMed]
8. Benisty, H.; de la Perrière, V.B.; Ramdane, A.; Lupu, A. Parity-Time Symmetric Gratings in 1550 nm Distributed-Feedback Laser Diodes: Insight on Device Design Rules. *J. Opt. Soc. Am. B* **2021**, *38*, C168–C174. [CrossRef]
9. Makris, K.G.; El-Ganainy, R.; Christodoulides, D.N.; Musslimani, Z.H. Beam Dynamics in PT Symmetric Optical Lattices. *Phys. Rev. Lett.* **2008**, *100*, 103904. [CrossRef] [PubMed]
10. Lin, Z.; Ramezani, H.; Eichelkraut, T.; Kottos, T.; Cao, H.; Christodoulides, D.N. Unidirectional Invisibility Induced by PT-Symmetric Periodic Structures. *Phys. Rev. Lett.* **2011**, *106*, 213901. [CrossRef] [PubMed]
11. Sun, Y.; Tan, W.; Li, H.; Li, J.; Chen, H. Experimental Demonstration of a Coherent Perfect Absorber with PT Phase Transition. *Phys. Rev. Lett.* **2014**, *112*, 143903. [CrossRef]
12. Wong, Z.J. Parity-Time Symmetric Laser and Absorber. In Proceedings of the 2018 Progress in Electromagnetics Research Symposium (PIERS-Toyama), Toyama, Japan, 1–4 August 2018. [CrossRef]
13. Phang, S. Theory and Numerical Modelling of Parity-Time Symmetric Structures for Photonics. Available online: http://eprints.nottingham.ac.uk/32596/ (accessed on 30 November 2018).
14. Mossakowska-Wyszyńska, A.; Witoński, P.; Szczepański, P. Operation of Fabry-Perot Laser with Nonlinear PT-Symmetric Mirror. *Bull. Pol. Acad. Sci. Tech. Sci.* **2021**, *69*, e139202. [CrossRef]
15. Witoński, P.; Mossakowska-Wyszyńska, A.; Szczepański, P. Effect of Nonlinear Loss and Gain in Multilayer PT-Symmetric Bragg Grating. *IEEE J. Quantum Electron.* **2017**, *53*, 8063405. [CrossRef]
16. Ge, L.; Chong, Y.D.; Stone, A.D. Conservation Relations and Anisotropic Transmission Resonances in One-Dimensional PT-Symmetric Photonic Heterostructures. *Phys. Rev. A* **2012**, *85*, 023802. [CrossRef]
17. Shramkova, O.V.; Tsironis, G.P. Resonant Combinatorial Frequency Generation Induced by a PT-Symmetric Periodic Layered Stack. *IEEE J. Sel. Top. Quantum Electron.* **2016**, *22*, 82–88. [CrossRef]
18. Pettit, G.D.; Turner, W.J. Refractive Index of InP. *J. Appl. Phys.* **1965**, *36*, 2081. [CrossRef]
19. Chong, Y.D.; Ge, L.; Stone, A.D. PT-Symmetry Breaking and Laser-Absorber Modes in Optical Scattering Systems. *Phys. Rev. Lett.* **2011**, *106*, 093902. [CrossRef] [PubMed]